# Electronic Structures of Transition Metal Phosphorus Monoxide Complexes

Attila Bérces, Olivia Koentjoro, Brian T. Sterenberg, John H. Yamamoto, John Tse, and Arthur J. Carty*

*Steacie Institute for Molecular Sciences, National Research Council of Canada, Ottawa, Ontario K1A 0R6, Canada*

*Received March 30, 2000*

Density functional theory calculations were carried out on the transition metal phosphorus monoxide complexes $(NH_2)_3MoPO$, $[\eta^5\text{-}C_5H_5Mo(CO)_2]_3PO$, $[\eta^5\text{-}C_5H_5W(CO)_2]_3PO$, $[Ru_4(CO)_{12}PO]^-$, $[Os_4(CO)_{12}PO]^-$, and $[Ru_5(CO)_{15}PO]^-$. The results indicate that $\pi$-bonding dominates the interaction of PO with transition metal clusters and that electrostatic effects, as well as orbital interactions, have a significant influence on the PO bond strength and can lead to IR frequencies above that of free PO.



## Introduction

Compared with the chemistry of its lighter congener NO, the coordination chemistry of phosphorus monoxide (PO) is not well developed. Unlike NO, PO is unstable relative to more highly oxidized phosphorus oxides, and the difficulty of accessing the molecule in the free state has hindered the establishment of extensive organometallic and coordination chemistry. In contrast however, PO has been extensively studied in matrices and in the gas phase by chemical physicists,[1] partly because it is thought to be the most abundant phosphorus-containing molecule in interstellar space.[2] A gas-phase equilibrium interatomic distance of 1.476370(15) Å has been measured using vibrational−rotational spectroscopy, while the PO stretching frequency in the free molecule has been measured as 1220.25 $cm^{-1}$ in the gas phase[3] and 1218 $cm^{-1}$ in matrices.[4]

The first PO cluster complex discovered was $(\eta^5\text{-}C_5HPr^i_4)_2Ni_2W(CO)_4(PO)_2$. This molecule was synthesized by the direct oxidation of the exposed phosphorus atoms of a coordinated $P_2$ molecule in the precursor $(\eta^5\text{-}C_5HPr^i_4)_2Ni_2W(CO)_4(P_2)$.[5] Similarly, oxidation of a $\mu_3$-phosphide complex was used to form the phosphorus monoxide clusters $[(Cp')_3Co_3(\mu_3\text{-}CC(CH_3)_3)(\mu_3\text{-}PO)]$ (Cp′ = $\eta^5\text{-}C_5H_4CH_2CH_2P(S)Bu^t_2$)[6] and $[\eta^5\text{-}C_5H_5(CO)_2Mo]_3PO$ as well as W and mixed MoW analogues of the latter.[7] The complex $[\{Cp''Co\}_3(\mu_3\text{-}PO)_2]$ (Cp″ = $\eta^5\text{-}C_5H_3Bu^t_2$-1,3), which contains two PO ligands, was formed by oxidation of the appropriate bis-phosphide complex,[8] while $[\{\eta^5\text{-}(CH_3)_5C_5Fe\}\{Cp''Co\}_2(\mu_3\text{-}PO)(\mu_4\text{-}P_2O)(\mu_2\text{-}P_2)]$ results from oxidation of $[\{\eta^5\text{-}(CH_3)_5C_5Fe\}\{Cp''Co\}_2(P_4)(P)]$.[9] The only example of a mononuclear PO complex, $(OP)Mo[N(R)Ar]_3$ (R = $C(CD_3)_2Me$, Ar = 3,5-$C_6H_3Me_2$), was formed by oxidation of the corresponding terminal phosphide complex.[10] With the description of a useful synthetic route to PO clusters via the hydrolysis of coordinated aminophosphinidene ligands,[11] a barrier to the synthesis of PO complexes has been removed and an extensive array of anionic PO clusters of Ru and Os have been synthesized.[12] Representative examples of PO complexes are shown in Chart 1.

In an effort to gain insight into the bonding of PO to transition metal clusters, we have compared PO bond lengths and $\nu$(PO) stretching frequencies. Bond length is the most direct experimentally measurable quantity related to bond strength. Vibrational stretching frequencies of ligands attached to transition metals are additional important indicators of bond strength. Since it is significantly easier to record the vibrational spectrum of a molecule than to determine the structure and the relative precision of vibrational frequencies is better than that of bond lengths, vibrational frequencies have

(1) (a) Ngo, T. A.; DaPaz, M.; Coquart, B. Couet C. *Can J. Phys.* **1974**, *52*, 154 (b) Ghosh, S. N.; Verma, R. D. *J. Mol. Spectrosc.* **1978**, 200 (c) Larzilliere, M.; Jacox, M. E. *J. Mol. Spectrosc.* **1980**, *79*, 132 (d) Kawaguchi, K.; Saito, S.; Hirota, E. *J. Chem. Phys.* **1983**, *79*, 629 (e) Verma, R. D.; McCarthy *Can. J. Phys.* **1983**, *61*, 1149 (f) Kawaguchi, K.; Saito, S.; Hirota, E.; Ohashi, N *J. Chem. Phys.* **1985**, *82*, 4893 (g) Hamilton, P. A. *J. Chem. Phys.* **1987**, *86*, 33 (h) Andrews, L.; Withnall, R. *J. Am. Chem. Soc.* **1988**, *110*, 5606 (i) Withnall, R.; Andrews, L. *J. Phys. Chem.* **1988**, *92*, 4610 (j) Withnall, R.; McCluskey, M.; Andrews, L. *J. Phys. Chem.* **1989**, *93*, 126 (k) Andrews, L.; McCluskey, M.; Mielke, Z.; Withnall, R.; *J. Mol. Struct.* **1990**, *222*, 95.

(2) Matthews, H. E.; Feldman, P. A. *Astrophys. J.* **1987**, *312*, 307.

(3) (a) Butler, J. E.; Kawaguchi, K.; Hirota, E. *J. Mol. Spectrosc.* **1983**, *101*, 161. (b) Qian, H.-B. *J. Mol. Spectrosc.* **1995**, *174*, 599.

(4) (a) Andrews, L.; McCluskey, M.; Mielke, Z.; Withnall, R. *J. Mol. Struct.* **1990**, *222*, 95. (b) Andrews, L.; Withnall, R. *J. Am. Chem. Soc.* **1988**, *110*, 5605.

(5) (a) Scherer, O. J.; Braun, J.; Walther, P.; Heckmann, G.; Wolmershäuser, G. *Angew. Chem., Int. Ed. Engl.* **1991**, *30*, 852 (b) Scherer, O. J.; Vondung, C.; Wolmershäuser, G. *Angew. Chem., Int. Ed. Engl.* **1997**, *36*, 1303.

(6) Foerstner, J.; Olbrich, F.; Butenschon, H. *Angew. Chem., Int. Ed. Engl.* **1996**, *35*, 1234.

(7) Davies, J. E.; Klunduk, M. C.; Mays, M. J.; Raithby, P. R.; Shields, G. P.; Tompkin, P. K. *J. Chem. Soc., Dalton Trans.* **1997**, 715.

(8) Scherer, O. J.; Weigel, S.; Wolmershäuser, G. *Heteroatom Chem.* **1999**, *10*, 622.

(9) Scherer, O. J.; Weigel, S.; Wolmershäuser, G. *Angew. Chem., Int. Ed.* **1999**, *38*, 3688.

(10) Johnson, M. J. A.; Odom, A. L.; Cummins, C. C. *J. Chem. Soc., Chem Commun.* **1997**, 1523.

(11) Corrigan, J. F.; Doherty, S.; Taylor, N. J.; Carty, A. J. *J. Am. Chem. Soc.* **1994**, *116*, 9799.

(12) (a) Wang, W.; Doherty, S.; Enright, G. D.; Taylor, N. J.; Carty, A. J. *Organometallics* **1996**, *15*, 2770 (b) Wang, W.; Carty, A. J. *New J. Chem.* **1997**, *21*, 773 (c) Wang, W.; Enright, G. D.; Driediger, J.; Carty, A. J. *J. Organomet. Chem.* **1997**, *541*, 461 (d) Yamamoto, J. H.; Udachin, K. A.; Enright, G. D.; Carty, A. J. *Chem. Commun.* **1998**, 2259. (d) Yamamoto, J. H.; Scoles, L.; Udachin, K. A.; Enright, G. D.; Carty, A. J. *J. Organomet. Chem.* **2000**, *600*, 54.

10.1021/om000274v CCC: $19.00 Published 2000 by the American Chemical Society
Publication on Web 09/22/2000

**Chart 1**

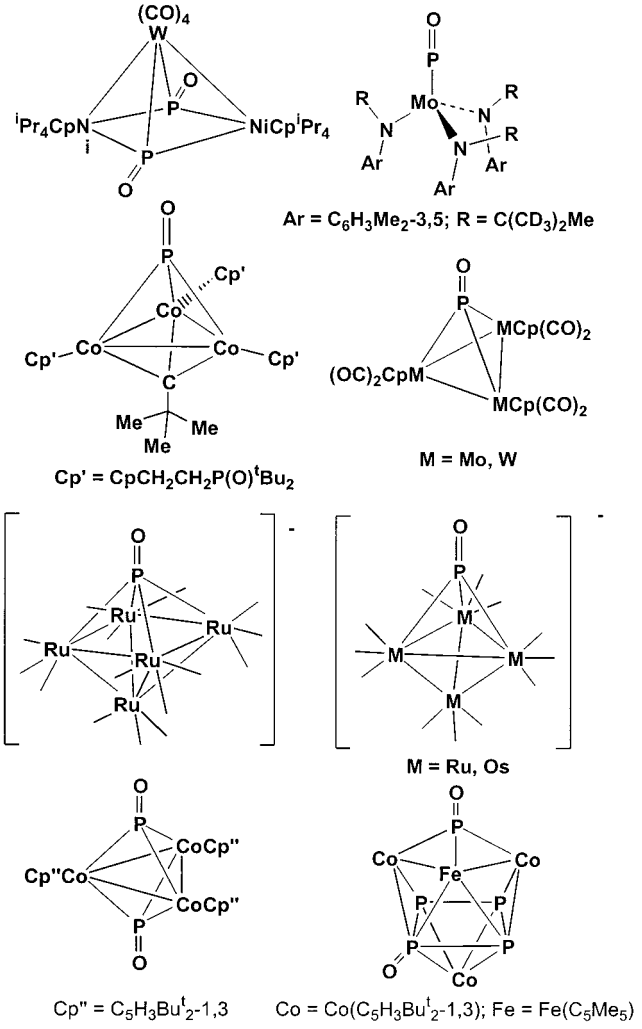


been a popular way to characterize bond strength. One challenge, however, is that assignment of the spectrum is not always straightforward. For metal carbonyls or nitrosyls, the IR bands are usually intense and appear in the spectrum well separated from other vibrational modes. On the other hand, $\nu$(PO) frequencies are usually weak and appear in a region of the spectrum (1000−1200 $cm^{-1}$) that frequently coincides with other vibrational modes.

We have surveyed the $\nu$(PO) frequencies and PO bond lengths in PO-containing complexes and have found a good linear correlation between these two quantities (Figure 1). Most PO frequencies fall below the 1220 $cm^{-1}$ of free PO, consistent with the expectation that donation into $\pi^*$ orbitals of PO reduces the bond strength. However, the PO stretching frequencies of $[\eta^5\text{-}C_5H_5M(CO)_2]_3PO$ (M = Mo, W)[6] occur well above that of free PO, at 1265 or 1266 $cm^{-1}$. In addition the only complex containing a terminal PO ligand, $Mo(PO)[NR(Ar)]_3$, also has a $\nu$(PO) value slightly above that of free PO.[9] It is not immediately clear why these $\nu$(PO) frequencies appear above that of free PO, although the observations are not unprecedented since it is known that in complexes of CS, the heavier congener of CO, $\nu$(CS) vibrational frequencies are often higher than in the uncomplexed ligands.[13]

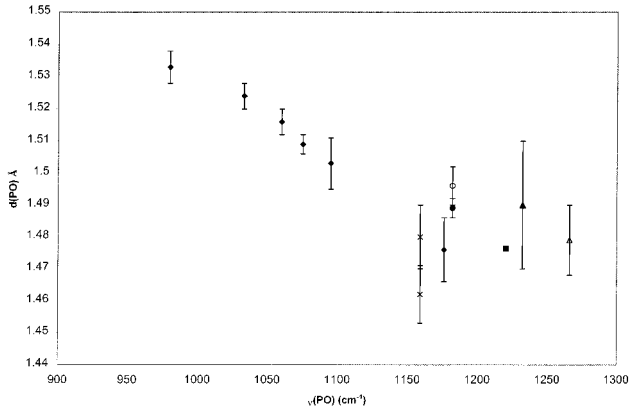


**Figure 1.** Correlation between $d$(PO) (Å) and $\nu$(PO) ($cm^{-1}$). The error bars correspond to the estimated standard deviations in the bond lengths. Legend: (◆) Ru and Os clusters, in order of increasing frequency: $[Ru_4(CO)_{12}Pt(PPh_3)(CO)(PO)][K]$, $[Ru_4(CO)_{12}Pt(PPh_3)(CO)(PO)][H_2NiPr_2]$, $[Os_4(CO)_{13}PO][Pr^i_2NH_2]$, $[Ru_5(CO)_{15}PO][Pr^i_2NH_2]$, $[Os_4(CO)_{12}PO][Et_4N]$, $[Ru_4(CO)_{12}PO][Pr^i_2NH_2]$; (×) $(\eta^5\text{-}C_5HPr^i_4)_2Ni_2W(CO)_4(PO)_2$; (●) $[\{Cp''Co\}_3(\mu_3\text{-}PO)_2]$ ($Cp'' = \eta^5\text{-}C_5H_3Bu^t_2$-1,3); (○) $[\{\eta^5\text{-}(CH_3)_5C_5Fe\}\{Cp''Co\}_2(\mu_3\text{-}PO)(\mu_4\text{-}P_2O)(\mu_2\text{-}P_2)]$; (■) free PO, (▲) (OP)Mo[N(R)Ar] (R = $C(CD_3)_2Me$, Ar = 3,5-$C_6H_3Me_2$); (△) $[\eta^5\text{-}C_5H_5(CO)_2Mo]_3PO$.

In an effort to explain the spectroscopic and structural data as well as to provide insights into the nature of M−PO bonding we have carried out electronic structure calculations based on density functional theory (DFT). We have selected a set of representative compounds, $(NH_2)_3MoPO$, $[\eta^5\text{-}C_5H_5Mo(CO)_2]_3PO$, $[\eta^5\text{-}C_5H_5W(CO)_2]_3PO$, and the cluster anions $[Ru_4(CO)_{12}PO]^-$, $[Os_4(CO)_{12}PO]^-$, and $[Ru_5(CO)_{15}PO]^-$ for a detailed theoretical study. The molecule $[\eta^5\text{-}C_5H_5Mo(CO)_2]_3PO$ contains a triply bridging PO ligand with distorted tetrahedral coordination at the phosphorus atom.[6] The anionic clusters $[Ru_4(CO)_{12}PO]^-$ and $[Os_4(CO)_{12}PO]^-$ exist with $[H_2NPr^i_2]^+$ and $[Et_4N]^+$ counterions and also have $\mu_3$ coordination of PO to a tetrahedral metal fragment.[10,12a] The molecule $(NH_2)_3MoPO$ is a theoretical model system for the observed mononuclear $Mo(PO)[NR(Ar)]_3$ (R = $C(CD_3)_2Me$, Ar = 3,5-$C_6H_3Me_2$), which possesses an $\eta^1$ terminal PO ligand.[9] Finally in $[Ru_5(CO)_{15}PO]^-$, which has been characterized with $[H_2N(Cy)_2]^+$ and $[H_2N(Pr^i)_2]^+$ counterions,[12d] the PO ligand is $\mu_4$ coordinated to the tetragonal face of a tetragonal pyramidal metal cluster. Our overall aim in this study is to qualitatively understand the bonding and to find a consistent explanation of the trends in vibrational frequencies.

## Computational Details

The reported calculations were carried out with the Amsterdam Density Functional (ADF) program system version 2.3 derived from the work of Baerends et al.[14] and developed at the Free University of Amsterdam[15] and at the University of Calgary.[16] All optimized geometries calculated in this study are based on the local density approximation[17] (LDA) aug-

(13) Woodward, S. S.; Jacobson, R. A.; Angelici, R. J. *J. Organomet. Chem.* **1976**, *117*, C75.
(14) Baerends, E. J.; Ellis, D. E.; Ros, P. *Chem. Phys.* **1973**, *2*, 41.
(15) (a) Ravenek, W. In *Algorithms and Applications on Vector and Parallel Computers;* te Riele, H. J. J., Dekker, Th. J., van de Vorst, H. A, Eds.; Elsevier: Amsterdam, 1987. (b) Boerrigter, P. M.; te Velde, G.; Baerends, E. J. *Int. J. Quantum Chem.* **1988**, *33*, 87. (c) te Velde, G.; Baerends, E. J. *J. Comput.Phys.* **1992**, *99*, 84.

mented with gradient corrections to the exchange[18] and correlation[17b] potentials. These calculations also include quasi-relativistic corrections to the Hamiltonian introduced by Snijders et al.[18] Schreckenbach et al. have implemented the analytic energy gradients based on quasi-relativistic DFT methods.[19]

We used an uncontracted triple-ζ Slater orbital basis set[20] with two polarization functions for the transition metals, phosphorus, and the oxygen of the PO ligand and a double-ζ basis set with one polarization function for all other atoms. The $1s^2$ configuration of carbon and oxygen and the $1s^22s^22p^6$ and $1s^22s^22p^63d^{10}$ configurations of second- and third-row transition metals, respectively, were assigned to the core and treated by the frozen-core approximation.[15] A set of auxiliary s, p, d, f, g, and h Slater functions, centered on all nuclei, was used to fit the molecular density and represent the Coulomb and exchange potentials accurately in each SCF cycle.[21]

The numerical integration accuracy parameter, which approximately represents the number of significant digits for the scalar matrix elements, was gradually increased to 4.5 until convergence with respect to integration accuracy was reached. These calculations were carried out on a multiprocessor SGI Origin 2000 computer. Gradient-corrected DFT calculations have been repeatedly shown to provide exceptionally good energetics for transition metal systems.[22]

## Results and Discussion

Our study of the bonding is based on a fragment orbital interaction analysis and consequent bond energy decomposition using a method developed by Ziegler and Rauk.[23] We describe four representative clusters, $(NH_2)_3$-MoPO, $[\eta^5\text{-}C_5H_5Mo(CO)_2]_3PO$, $[Ru_4(CO)_{12}PO]^-$, and $[Ru_5(CO)_{15}PO]^-$. This set represents both neutral and anionic clusters with $\eta^1$, $\eta^3$, and $\eta^4$ bridging coordination modes. All clusters have $C_{3v}$ point group symmetry with the exception of the $C_s$ symmetry cluster $[Ru_5(CO)_{15}PO]^-$. The symmetry labeling and orbital numbering refer to the results of our DFT calculations.

Before examining the PO ligand itself, it is worth considering two better studied ligands, CO and NO. The inverse correlation between CO stretching frequency and $\pi$ back-bonding for most metal carbonyls is a well-known textbook example.[24] Electron donation from filled

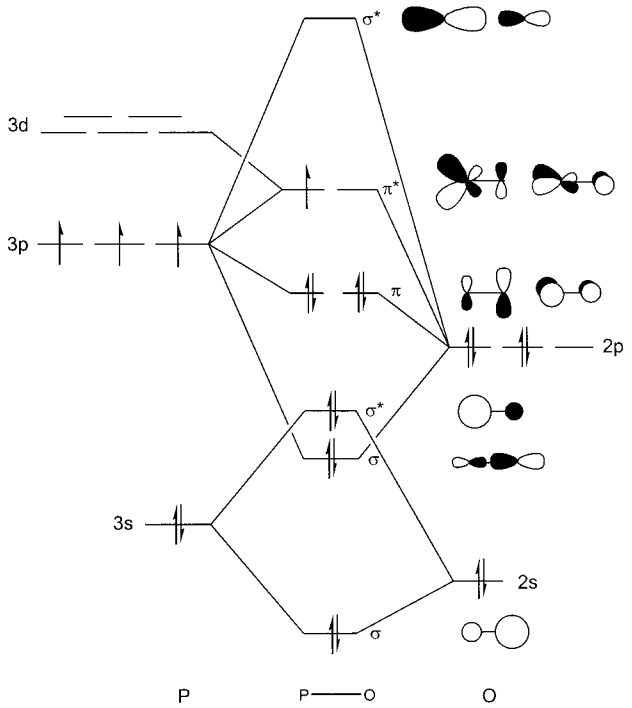


**Figure 2.** Schematic representation of the MO diagram of PO.

metal d orbitals into the lowest unoccupied $\pi^*$ orbital of CO is the dominant interaction in most metal carbonyl complexes, a fact that nicely explains the correlation. The electronic structure of NO differs from that of CO by an additional electron in the $\pi^*$ antibonding orbital which is fairly readily lost to give the nitrosonium ion $NO^+$ ($\Delta H_{ion}$ = 891 kJ/mol).[25] The nitrosonium ion is isoelectronic with CO and has a shorter bond length and higher vibrational frequency than NO. The coordination of NO to transition metals often involves the donation of the $\pi^*$ electron to the metal d orbitals, and in these compounds the properties of the NO ligand resemble those of $NO^+$. The partially occupied $\pi^*$ orbital can act not only as a donor but also as an acceptor, and there is spectroscopic evidence that NO is a good $\pi$ acceptor.[26] When NO acts as an acceptor, its properties resemble those of $NO^-$. Due to the versatility of the binding modes of the nitrosyl ligand, the NO stretching vibrational frequencies of terminal metal nitrosyls range from ~1500 to 2000 $cm^{-1}$. The valence electronic structures of PO and NO are similar with the exception of the higher principal quantum numbers of the valence orbitals of phosphorus. The comparison with NO is particularly useful since the coordination chemistry of NO is well understood.

The schematic orbital interaction diagram of PO indicates that the highest occupied $\sigma$ orbital is an antibonding combination of the 3s and the 2s orbitals of phosphorus and oxygen, respectively (see Figure 2). Our DFT calculations indicate that the s-type and the p-type $\sigma$ orbitals do not separate into a pair of strongly antibonding and strongly bonding components as shown on the schematic interaction diagram of Figure 2, but are better described as sp hybrid orbitals of mainly

(16) (a) Fan, L.; Ziegler, T. *J. Chem. Phys.* **1991**, *94*, 6057. (b) Fan, L.; Ziegler, T. *J. Chem. Phys.* **1991**, *95*, 7401. (c) Fan, L.; Versluis, L.; Ziegler, T.; Baerends, E. J.; Ravenek, W. *Int. J. Quantum Chem.* **1988**, *S22*, 173. (d) Fan, L.; Ziegler, T. *J. Chem. Phys.* **1992**, *96*, 9005. (e) Fan, L.; Ziegler, T. *J. Phys. Chem.* **1992**, *96*, 6937.

(17) (a) Vosko, S. H.; Wilk, L.; Nusair, M. *Can. J. Phys.* **1980**, *58*, 1200. (b) Becke, A. D. *Phys. Rev. A* **1988**, *38*, 2398. (c) Perdew, J. P. *Phys. Rev. B* **1986**, *33*, 8822. (d) Perdew, J. P. *Phys. Rev. B* **1986**, *34*, 7046.

(18) (a) Snijders, J. G.; Baerends, E. J.; Ros, P. *Mol. Phys.* **1978**, *36*, 1789. (b) Snijders, J. G.; Baerends, E. J.; Ros, P. *Mol. Phys.* **1979**, *36*, 1969.

(19) Schreckenbach, G.; Ziegler, T.; Li, J. *Int. J. Quantum Chem., Quantum Chem.* **1995**, *56*, 477.

(20) (a) Snijders, G. J.; Baerends, E. J.; Vernooijs, P. *At. Nucl. Data Tables* **1982**, *26*, 483. (b) Vernooijs, P.; Snijders, G. J.; Baerends, E. J. *Slater Type Basis Functions for the Whole Periodic System*; Internal Report; Free University of Amsterdam: The Netherlands, 1981.

(21) Krijn, J.; Baerends, E. J. *Fit Functions in the HFS-Method;* Internal Report (in Dutch); Free University of Amsterdam: The Netherlands, 1984.

(22) Ziegler, T. *Chem. Rev.* **1991**, *91*, 651.

(23) (a) Ziegler, T.; Rauk, A. *Theor. Chim. Acta* **1977**, *46*, 1. (b) Ziegler, T. *A General Energy Decomposition Scheme for the Study of Metal−Ligand Interactions in Complexes, Clusters and Solids*; NATO ASI, in press. (c) Ziegler, T.; Rauk, A. *Inorg. Chem.* **1979**, *18*, 1558. (d) Ziegler, T.; Rauk, A. *Inorg. Chem.* **1979**, *18*, 1755.

(24) Collman, J. P.; Hegedus, L. S.; Norton, J. R.; Finke R. G. *Principles and Applications of Organotransition Metal Chemistry*; University Science Books: Mill Valley, CA, 1987; p 114.

(25) Cotton, F. A.; Wilkinson, G. *Advanced Inorganic Chemistry*; John Wiley & Sons: New York 1988; p 322.

(26) Griffith, W. P. *Adv. Organomet. Chem.* **1968**, *7*, 211−239.

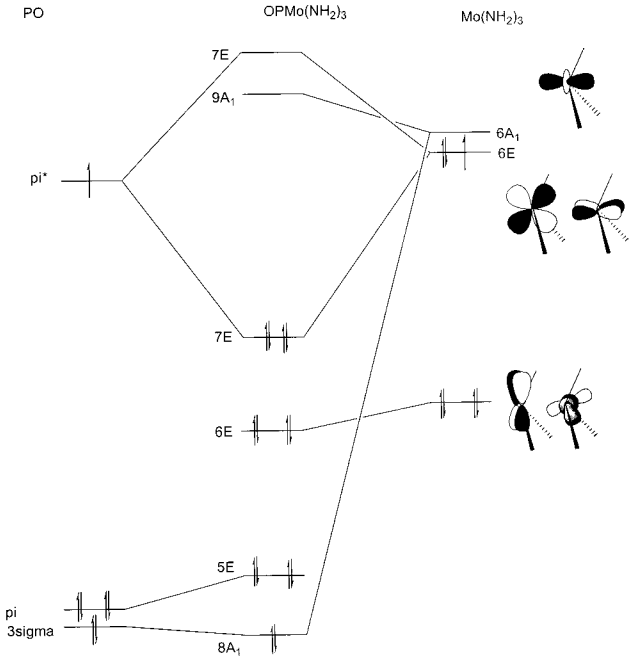


**Figure 3.** Orbital interaction diagram of $(NH_2)_3MoPO$.

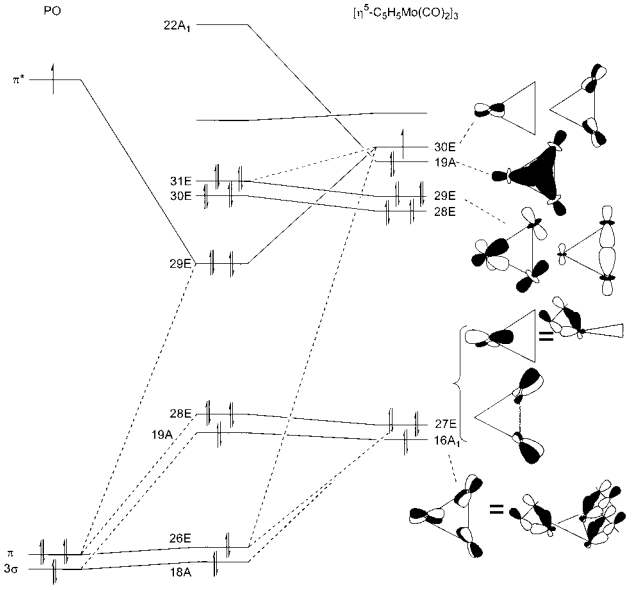


**Figure 4.** Orbital interaction diagram of $[\eta^5\text{-}C_5H_5Mo(CO)_2]_3PO$.

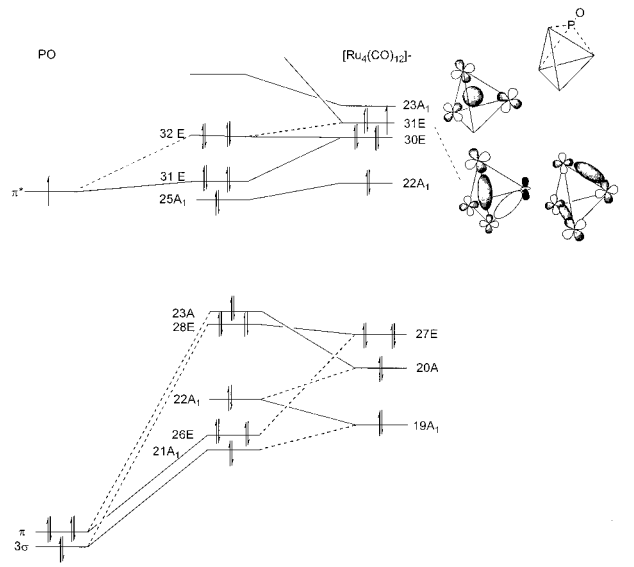


**Figure 5.** Orbital interaction diagram of $[Ru_4(CO)_{12}PO]^-$.

nonbonding character. The nature of these orbitals is sensitive to the overlap between atomic orbitals and consequently to the PO bond length. The bonding character of the highest $\sigma$ orbital increases with increasing PO bond length.

When comparing NO and PO, we should also point out the differences resulting from the availability of the low lying 3d orbital of the phosphorus. The $\pi^*$ orbital of NO is strongly antibonding, and electron acceptance reduces the NO bond strength substantially. The stretching frequency of $NO^-$ is reduced by 514 $cm^{-1}$, compared to NO. The $\pi^*$ of PO has a weaker antibonding character due to mixing in of the d orbital, and uptake of an electron reduces the PO stretching frequency by only 205 $cm^{-1}$, based on our DFT calculations.

**Orbital Interactions in Transition Metal Complexes.** The interaction diagram of the mononuclear $(NH_2)_3MoPO$ complex (Figure 3) is very simple. The $\pi^*$ orbital of PO and the molybdenum-based, essentially $d_{xz}$ and $d_{yz}$ degenerate orbital pair of E symmetry form a stable bonding combination. Since these two orbitals are occupied by a total of four electrons, the maximum occupation for the degenerate E orbitals, this interaction leads to a strong stabilization. The unoccupied $6A_1$ orbital of $(NH_2)_3MoPO$, which can be characterized as the $d_{z^2}$ of Mo, interacts with the $3\sigma$ orbital of PO. This interaction is responsible for the $\sigma$ donation from PO to the metal.

The orbital interaction diagram of $[\eta^5\text{-}C_5H_5Mo(CO)_2]_3PO$ (Figure 4) shows one particularly strong stabilizing interaction between the $\pi^*$ of PO and the 30E HOMO orbital of $[\eta^5\text{-}C_5H_5Mo(CO)_2]_3$ that forms the 29E MO of $[\eta^5\text{-}C_5H_5Mo(CO)_2]_3PO$. There is also a small but significant mixing of the $\pi$ orbital into the 29E bonding orbital, which will be addressed shortly. The degenerate 29E orbital is occupied by four electrons: two electrons come from the fragment orbitals and another two electrons from the $19A_1$ orbital of $[\eta^5\text{-}C_5H_5Mo(CO)_2]_3$, which is destabilized and pushed above the highest occupied level. The $\pi$ and $3\sigma$ orbitals of PO form bonding and antibonding combinations with the 27E and $16A_1$ fragment orbitals, respectively, which leads to a net repulsive interaction. The cyclopentadienyl ligands make significant contributions to the 27E and $16A_1$ cluster orbitals, which can be regarded as the $A_1$ and E combinations of the three metal−Cp bonding orbitals.

The orbital interaction diagram of $[Ru_4(CO)_{12}PO]^-$ (Figure 5) also shows some attractive $\pi$ interactions similar to that of $[\eta^5\text{-}C_5H_5Mo(CO)_2]_3PO$. However, we cannot pinpoint any one particularly strong stabilizing interaction. Two sets of E orbitals, the filled 30E and the partly filled 31E orbitals of $[Ru_4(CO)_{12}]^-$, are stabilized upon interactions with the partly filled $\pi^*$ orbital of PO. In contrast with $[\eta^5\text{-}C_5H_5Mo(CO)_2]_3PO$, however, there is no evidence of strong mixing of $\pi$ and $\pi^*$ orbitals of PO in $[Ru_4(CO)_{12}PO]^-$. In addition to the $\pi$ interactions, the $22A_1$ orbital of $[Ru_4(CO)_{12}]^-$ is stabilized without any significant orbital interactions, which we explain as the result of an electrostatic effect.

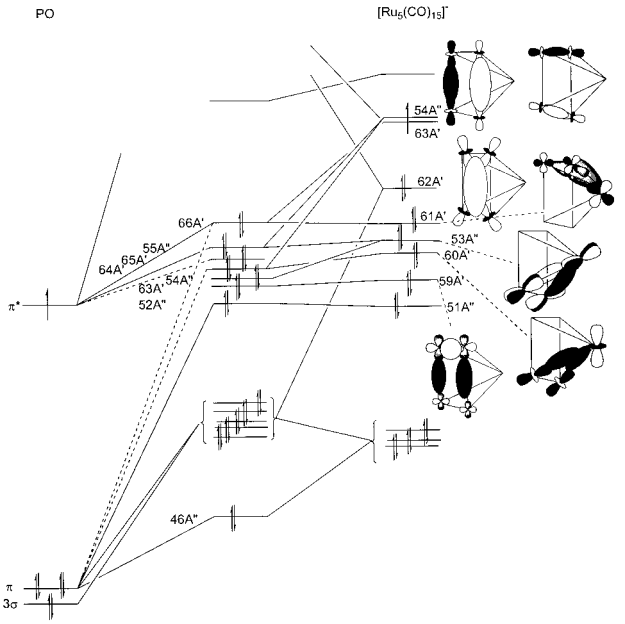


**Figure 6.** Orbital interaction diagram of $[Ru_5(CO)_{15}PO]^-$.

The $\pi$ and $3\sigma$ orbitals of PO lead to some repulsive interactions with the metal orbitals of appropriate symmetry.

The orbital interaction diagram of $[Ru_5(CO)_{15}PO]^-$ (Figure 6) is conceptually very similar to that of $[Ru_4(CO)_{12}PO]^-$. The $\pi^*$ orbital stabilizes four sets of high lying cluster orbitals. The strength of the interaction comes from small stabilizing interactions with several orbitals instead of one strong interaction with one particular orbital, as is the case for $[\eta^5\text{-}C_5H_5Mo(CO)_2]_3PO$ or $(NH_2)_3MoPO$.

**Vibrational Frequencies.** Density functional theory has been very successful in reproducing observed vibrational frequencies of transition metal compounds.[27] PO, however, seems to be less accurately described by gradient-corrected density functional theory. DFT at a generalized gradient approximation level using a triple-$\zeta$ basis set with double polarization functions seriously overestimates the PO bond length at 1.513 Å as opposed to the experimental value of 1.476 Å. The corresponding calculated PO stretching frequency is 1165 $cm^{-1}$, significantly lower than the experimental 1220 $cm^{-1}$. By contrast, the same level of theory can reproduce harmonic vibrational frequencies of nickel, iron, and chromium carbonyls with an average error of a few $cm^{-1}$ and M−C and C−O distances within a few milliangstroms of the experimental values.[28] Partial inclusion of Hartree−Fock exchange improves the PO results but does not rectify the problem. The total binding energy and the bond strength are determined by small differences between large attractive and repulsive energy terms. Even a relatively small error in one term can lead to a serious error in the PO bond length and the vibrational frequency. This seems to be the case with PO and PO-containing transition metal clusters. Table 1 compares the experimental and the calculated PO distances for a variety of PO clusters. The discrepancy between the experiment and the theory can partly be explained by the difference in the theoretical model and the experimental conditions. The theoretical calculation always refers to the gas phase structure, while the experimental structures come from the solid state, and in the case of anionic structures, the anions crystallize in the lattice. Counterion interactions, especially hydrogen bonding between PO and the counterion, as well as packing forces in the lattice have a significant effect on the PO bond length, but these effects are unaccounted for in the theoretical calculations. For these reasons, we cannot expect quantitative agreement between the experimental and theoretical structural parameters. Thus our aim has been to understand the orbital and electrostatic interactions between PO and transition metal centers and to study how these interactions affect the physical and chemical properties of these systems.

Our survey of $\nu$(PO) in metal−PO compounds shows a range of vibrational frequencies both above and below that of free PO. By analogy with NO, one would expect that the high values of $\nu$(PO) could be attributed to a coordination mode where PO acts as a $\pi$ donor and its structural and spectroscopic properties resemble that of $PO^+$. Since negatively charged clusters show lower $\nu$(PO) values, it is reasonable to think that PO carries a significant portion of this negative charge and acts like $PO^-$ in these systems. Electronic structure calculations can give an insight into the charge distribution and test the validity of these assumptions. The Hirshfeld charge analysis is a particularly convenient way to analyze charge transfer.[29] In this analysis, the electron density of the compounds at any given point in space is divided into fragment densities in the ratio of the contribution of the fragments to the superposition of fragment densities. The Hirshfeld analysis is sensitive to the reference electron configuration of the interacting fragments. The orbital interaction diagram of $[\eta^5\text{-}C_5H_5Mo(CO)_2]_3PO$ shows that the ground state electron configuration of the fragment $[\eta^5\text{-}C_5H_5Mo(CO)_2]_3$ does not correspond to the electron configuration of $[\eta^5\text{-}C_5H_5Mo(CO)_2]_3PO$ since the occupied $19A_1$ fragment orbital is destabilized and becomes unoccupied upon interaction with PO. To be consistent in our comparative study of electron transfer, we carried out the Hirshfeld analysis using a fragment electron configuration that corresponds to the electron population in the ground state of the combined fragments. The total charge transferred to PO (Table 1) ranges between −0.09 for $[Ru_5(CO)_{15}PO]^-$ and −0.37 for $[\eta^5\text{-}C_5H_5W(CO)]_3PO$ based on our Hirshfeld analysis. These results conclusively show that while the oxygen atom of the PO ligand in these clusters carries more negative charge, the resonance form $M_nP-O^-$, where a full negative charge is localized on oxygen, is not a good representation of the PO ligand in the anionic clusters. Indeed the neutral complexes donate more electron density to PO than the anionic clusters. In addition, there is no evidence of charge transfer to the metal from PO in any of the systems studied and the high $\nu$(PO) values of the neutral clusters cannot be explained by a $PO^+$ coordination mode. Thus, the different spectroscopic characteristics of the PO ligand

(27) Berces, A.; Ziegler, T. In *Topics in Current Chemistry: Density Functional Theory*; Nalewajski, R. F., Ed.; Springer-Verlag: Berlin, 1996; pp 41−88.

(28) Berces, A.; Ziegler, T. *J. Phys. Chem.* **1995**, *99*, 11417−11423.

(29) (a) Hirshfeld, F. L. *Theor. Chim. Acta* **1977**, *44*, 129. (b) Wiberg, K. B.; Rablen, P. R. *J. Comput. Chem.* **1993**, *14*, 1504.

**Table 1. Results of DFT Calculations: PO Bond Length, Charge Transfer to PO, Mulliken Population Gain of PO $\sigma$ and $\pi$ Orbitals**

| | $d$(PO) (Å) | | charge transfer by Hirschfeld analysis | | Mulliken charges | | | | population analysis | | | orbital interaction energy (kJ/mol) | |
|---|---|---|---|---|---|---|---|---|---|---|---|---|---|
| compound | calcd | exp | PO | cluster | $M_{eq}$ | $M_{ax}$ | P | O | 3d (P) | 3$\sigma$ (PO) | $\pi$* (PO) | $A_1$ | E |
| PO | 1.513 | 1.476 | | | | | 0.37 | −0.37 | 0.25 | 2.0 | 0.50 | | |
| $[Ru_4(CO)_{12}PO]^-$ | 1.510 | 1.509[a] | −0.19 | −0.81 | 1.01 | 0.98 | −0.18 | −0.48 | 0.84 | 1.83 | 0.78 | −497 | −1792 |
| $[Os_4(CO)_{12}PO]^-$ | 1.510 | 1.476 | −0.21 | −0.79 | 0.94 | 0.93 | −0.07 | −0.49 | 0.83 | 1.81 | 0.78 | −272 | −1478 |
| $[CpMo(CO)_2]_3PO$ | 1.538 | 1.479 | −0.35 | 0.35 | 1.88 | | 0.17 | −0.54 | 0.77 | 1.81 | 0.86 | −363 | −1723 |
| $[CpW(CO)_2]_3PO$ | 1.538 | | −0.37 | 0.37 | 1.78 | | 0.17 | −0.55 | 0.78 | 1.83 | 0.88 | −301 | −1607 |
| $(NH_2)_3MoPO$ | 1.516 | 1.49 | −0.28 | 0.28 | 1.78 | | 0.11 | −0.60 | 0.56 | 1.74 | 0.81 | −158 | −886 |
| $[Ru_5(CO)_{15}PO]^-$ | 1.521 | 1.516 | −0.09 | −0.91 | 0.98 | 0.94 0.86 | −0.21 | −0.50 | 0.86 | 1.80 | 0.82 (0.79) | *b* | |

[a] The solid-state structure of $[H_2NPr^i_2][Ru_4(CO)_{12}PO]$ exhibits hydrogen bonding between the cation and the oxygen of the PO ligand, resulting in a lengthening of the PO bond. [b] In $C_s$ symmetry the orbital interactions cannot be separated into $\sigma$ and $\pi$ components.

in the neutral and anionic clusters cannot be attributed to the total charge.[30]

High vibrational frequencies of diatomic ligands can also be a result of $\sigma$ donation from an antibonding $\sigma$* orbital to the metal center. However, as we have shown in the previous section, the highest filled $\sigma$* orbital does not have significant antibonding character but is close to nonbonding. Thus, the $\sigma$ bonding does not affect the vibrational frequencies of PO significantly.

We can gain additional insight into the extent of $\sigma$ and $\pi$ donation from Mulliken electron population analysis.[31] The total charge transfer is the balance between the $\sigma$ donation from PO to the metal and the $\pi$ back-donation from the metal to PO. The $\sigma$ donation in all systems is uniform and amounts to the transfer of ~0.2 electron from the highest $\sigma$ orbital of PO to the metal cluster, except in $(NH_2)_3MoPO$, where the $\sigma$ donation is more substantial (0.26 electron). This can be explained by the better overlap between the metal- and PO-based $\sigma$ orbitals in the linear geometry. The population gain (or electron acceptance) of the $\pi$* orbital of PO ranges from 0.8 to 0.9 electron including both degenerate components. Our analysis enables the calculation of the interaction energies associated with different types of bonds. The interaction energy of the $\pi$ orbitals (Table 1) is more substantial than that of $\sigma$ orbitals. Therefore, measured both by interaction energies and the amount of charge transfer, $\pi$ bonding is more important than $\sigma$.

There is some discrepancy between the sum of the $\sigma$ and $\pi$ charge transfers of the Mulliken population analysis and the net charge transfer calculated by Hirshfeld analysis. This is partly explained by the different philosophies applied to assign electron density to atoms and orbitals by the two methods. In addition, our model does not account for the change in the character of the orbitals. For example, we assume that the $\pi$* orbital of PO mixes only with orbitals of the metal fragments but do not consider that the composition of the $\pi$* orbital may also change. However, such a change in the composition of the orbitals is apparent when we consider the participation of the d orbital of phosphorus in the $\pi$ and $\pi$* orbitals. Mulliken population analysis also allows us to monitor the contribution of d orbitals to the occupied orbitals by calculating the d electron population of phosphorus. In free PO, the d population is only 0.25 electron, while in the cluster compounds it ranges as high as 0.95. This large change in the d population suggests that the composition of the highest energy orbitals, especially the $\pi$*, changes significantly when PO interacts with transition metals. In our analysis such rehybridization is accounted for as electron transfer from an occupied PO orbital to an unoccupied PO orbital.

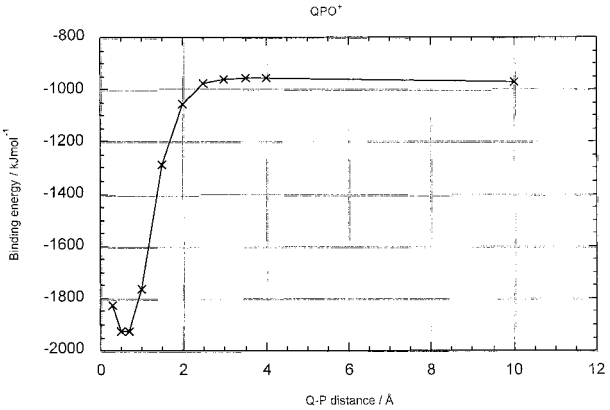


**Figure 7.** Binding energy of $QPO^+$ in the presence of a unit charge at different distances. 10 Å value corresponds to the PO bond distance without charge present.

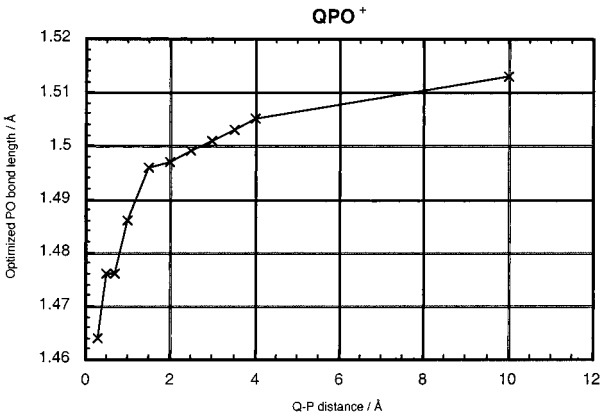


**Figure 8.** Effect of approaching unit positive charge on the equilibrium PO bond length. 10 Å value corresponds to the PO bond distance without charge present.

(30) A referee has pointed out the apparent discrepancy between the results of the Hirshfeld analysis and the Mulliken analysis and has questioned the use of the former. However the two methods provide complementary and useful information. The Hirshfeld analysis better reflects actual electron density flow upon binding since it uses the electron density of the interacting fragments as a weighting factor for the assignment of charge to particular fragments. Clearly, the results must be used cautiously, and we limit our analysis of the Hirschfeld results to eliminating the possibility of $PO^-$ and $PO^+$ coordination modes in the clusters.

(31) Mulliken, R. S. *J. Chem. Phys.* **1955**, *23*, 1833.

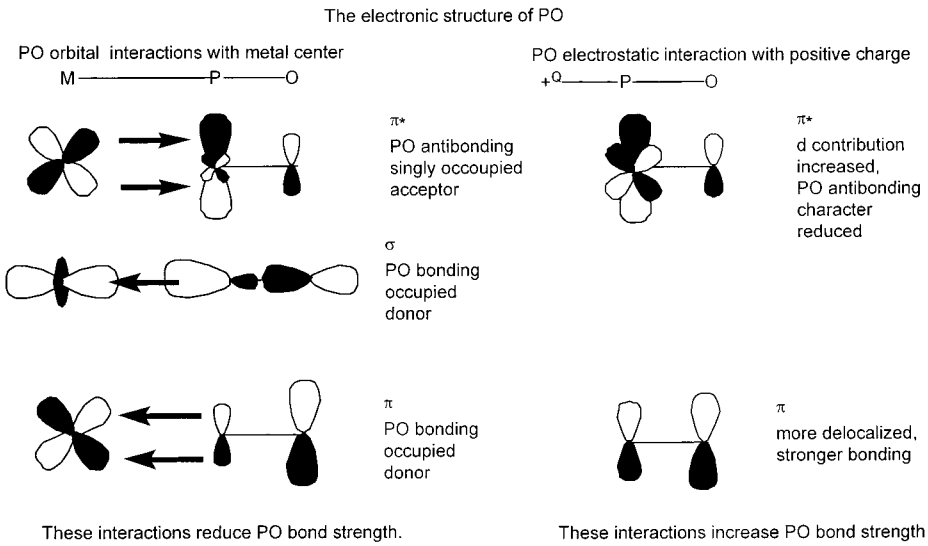


**Figure 9.** Effect of orbital and electrostatic interactions on the high-energy orbitals of PO. An exaggerated drawing.



Another mechanism for the change in the orbital composition is a difference in the orbital polarization. This does not require a higher empty orbital involvement, such as a d contribution. The $\pi$ orbital of PO is polarized toward the oxygen which is responsible for the net negative charge on the oxygen. The $\pi^*$ orbital, on the other hand, carries a disproportionately higher weight on the phosphorus. Upon interacting with the metal fragments, the $\pi$ and $\pi^*$ orbitals can mix and affect the polarity of both orbitals. We see evidence of such orbital mixing in the orbital diagram of $[\eta^5\text{-}C_5H_5\text{-}Mo(CO)_2]_3PO$ mentioned previously. The mixing of the orbitals of the same fragment is the result of the interaction of these orbitals in the presence of the electrostatic field of the other fragment. In search of an explanation for the high $\nu$(PO) of neutral PO-containing metal clusters, we examined how this electrostatic polarization effect might influence the PO bond strength.

The metal centers in all of the clusters discussed here are positively charged, so we must look at the interaction of the positive charge as it approaches PO from the phosphorus end. At first sight, this does not seem to be a promising mechanism for explaining the stabilization of the PO bond. The PO dipole is positively charged at the phosphorus end, and the approach of another positive charge leads to a repulsive interaction. The binding energy of PO as a function of the distance from a positive unit charge (Figure 7) shows that at large distances the interaction is weakly repulsive, but in the typical range of metal−ligand bonding the interaction is strongly attractive. The effect of the positive charge on the equilibrium PO distance is shown in Figure 8, and a schematic representation of the orbital interactions of PO with a transition metal and with a positive point charge is shown in Figure 9. The attractive interaction can be rationalized by the polarization of the electron cloud of PO by the positive charge and the resulting effective increase of the electronegativity of phosphorus. The $\pi$ orbital, which is strongly polarized toward oxygen, becomes more evenly distributed and thus more bonding. In addition to the polarization, the positive charge induces a rehybridization of the phosphorus orbitals with an increase of the d character in the $\pi^*$ orbitals. The d orbital is bonding with respect to the p orbital of oxygen in the $\pi^*$ MO; thus, this hybridization reduces the antibonding character of the $\pi^*$ orbital. The effect of the positive charge on both the $\pi$ and the $\pi^*$ orbitals is to increase the PO bond strength.

Although the mechanism of the increased bond strength of PO upon interaction with a point charge is unique, a similar effect of metal charge on ligand bond strength has been documented for CO. Indeed, an increasing number of carbonyl complexes are known with CO stretching vibrational frequencies above that of free CO.[32] Goldman and Krogh-Jespersen have shown that the high $\nu$(CO) values of carbonyl complexes can be explained by electrostatic effects due to the positive charge on the metal center and not to $\sigma$-bonding as previously thought.[33] Lupinetti and co-workers showed that the equilibrium CO bond length increases first, reaches a turning point, and then decreases as a positively charged transition metal approaches a CO ligand from the C terminus.[34] Consequently, $\nu$(CO) frequencies or C−O bond lengths of carbonyl complexes cannot be directly correlated with the metal−carbon bond strength when the metal is positively charged.

Model calculations with a unit charge placed between 2.0 and 2.5 Å from the P end of PO have shown that the PO frequency can increase by as much as 35 $cm^{-1}$ due to electrostatic effects. We have also found that the effect of three partial positive point charges placed in a triangle perpendicular to the PO bond has an effect similar to the sum of these charges placed in collinear orientation. When PO is coordinated to triangular or tetragonal faces of positively charged metal clusters, the combined polarization effects can be quite substantial and partially or fully compensate for the effect of orbital

(32) (a) Weber, L. *Angew. Chem., Int. Ed. Engl.* **1994**, *33*, 1077. (b) Rack, J. J.; Webb, J. D.; Strauss, S. H. *Inorg. Chem.* **1996**, *35*, 277. (c) Aubke, F.; Wang, C. *Coord. Chem. Rev.* **1994**, *137*, 483, and references therein. (d) Willner, H.; Bodenbinder, M.; Wang, C.; Aubke, F. *J. Chem. Soc., Chem. Commun.* **1994**, 1189. (e) Wang, C.; Bley, B.; Balzer-Jollenbeck, G.; Lewis, A. R.; Willner, H.; Aubke, F. *J. Chem. Soc., Chem. Commun.* **1995**, 2071.

(33) Goldman, A. S.; Krogh-Jespersen, K. *J. Am. Chem. Soc.* **1996**, *118*, 12159.

(34) (a) Lupinetti, A. J.; Fau, S.; Frenking, G.; Strauss, S. H. *J. Phys. Chem. A* **1997**, *101*, 9551. (b) Lupinetti, A. J.; Frenking, G.; Strauss, S. H. *Angew. Chem., Int. Ed.* **1998**, *37*, 2113-2116.

interactions on the PO bond strength. The highest positive vibrational frequency shift, 46 $cm^{-1}$ relative to free PO, was observed for $[\eta^5\text{-}C_5H_5Mo(CO)_2]_3PO$. The calculated Mulliken charge on the Mo atoms of this cluster is 1.9, the highest among the systems studied theoretically. Effectively, the metal center in the neutral clusters has a higher oxidation number due to the negatively charged cyclopentadienyl ligand. We find that the polarization effect from the positive charge is the only reasonable explanation for the blue-shift of the PO stretching frequency upon coordination to a transition metal center or cluster fragment.

## Conclusions

The orbital interactions between PO and transition metals are dominated by $\pi$ back-bonding regardless of the coordination mode, the metal oxidation state, or the type of transition metal. The $\sigma$ orbital makes a less significant contribution to bonding than the $\pi$ orbital. Our population analysis shows that the negative charge on the anionic clusters is not localized on the PO ligand. A positive charge on the metal center polarizes the PO orbitals, which increases the d component in the $\pi^*$ orbital and increases the weight of the phosphorus p orbitals in the $\pi$ orbital. Both of these effects increase the PO bond strength. Thus, the bond strength, the bond length, and the ligand stretching vibrational frequencies of PO ligands attached to transition metal clusters are determined not only by the orbital interaction between the metal and PO but also by the electrostatic interaction from the charge of the transition metal. The effect of positive charge is similar in magnitude but opposite in effect to orbital interactions, and the balance strongly depends on the oxidation state of the metal. In clusters with metals in high oxidation states, the charge polarization effect becomes dominant and $\nu$(PO) can be higher than the 1220 $cm^{-1}$ value corresponding to the PO radical. The interactions of PO and NO with transition metals are very different despite their apparently similar valence electronic structures. The availability of the d electrons to participate in bonding makes a significant contribution to the properties and the chemistry of PO.

**Acknowledgment.** We thank the Natural Sciences and Engineering Research Council of Canada and the National Research Council for financial support.

OM000274V